Dynamic Rupture on Rough Faults and Production of High-Frequency Radiation

David Belanger [1] and Eric M. Dunham [2,3]
belang@fas.harvard.edu edunham@fas.harvard.edu

(1) Department of Mathematics, Harvard University; (2) Department of Earth and Planetary Sciences, Harvard University; (3) Division of Engineering and Applied Sciences, Harvard University

Abstract

We have developed a highly accurate 2D finite difference method to solve dynamic rupture problems in irregular geometries. Our objective is to connect properties of high frequency radiation produced during slip on rough faults to statistical measures of fault roughness (namely, the amplitude-to-wavelength ratio, γ, of self-similar fractal faults). We study differences between antiplane and in-plane propagation; while faults are rougher in the direction perpendicular to slip ($\gamma = 10^{-2}$ vs. 10^{-3} in the slip direction), only in the in-plane case does slip on rough faults alter the normal stress. Antiplane propagation is only mildly perturbed at $\gamma = 10^{-2}$, suggesting that it might be possible to construct approximate broadband seismograms as the sum of the wavefield from slip on a flat fault plus a first-order correction term to account for roughness. The changes in normal stress in the in-plane case can dramatically influence the rupture process; in some cases, conditions that permit propagation on flat faults are insufficient to host ruptures on rough faults. To handle irregular geometries, we transform the governing equations from a non-Cartesian coordinate system that conforms to the irregular boundaries of the physical domain to a Cartesian coordinate system in a rectangular computational domain, and solve the equations in the computational domain. To accurately capture the high frequency wavefield, we use a numerical method that produces far smaller oscillations than those plaguing conventional finite difference/element methods. The governing equations (momentum conservation and Hooke's law) are written as a system of first-order equations for velocity and stress, which are defined at a common set of grid points and time steps (i.e., there is no staggering in space or time). Time stepping is done using an explicit third-order Runge-Kutta method. The equations are hyperbolic and the fields can be decomposed into a set of waves (with associated wave speeds). Spatial derivatives are computed with fifth-order WENO (weighted essentially non-oscillatory) finite differences in the upwind direction associated with each wave [Jiang and Shu, J. Comp. Phys., 126(1), 202-228, 1996]. Rather than using data from a single stencil (i.e., set of grid points) to calculate the derivative, a weighted combination of data from several candidate stencils is used. The weights are assigned based on solution smoothness within each stencil, and stencils in which the solution exhibits excessive variations are given minimal weight. Consequently, numerical oscillations are suppressed, even in the vicinity of the rupture front and at wavefronts.

Motivation

Target Problem: Connect Fault Roughness to High Frequency Ground Motion

Stochastic rupture models (with heterogeneous stresses, for example) are widely used to decrease coherence of rupture process and generate high frequency ground motion. However, those models are applied on planar faults, and one often considers heterogeneous stress or strength on a flat fault as a proxy for unmodeled geometrical heterogeneities. With proper tools, we can investigate this problem more rigorously. Since high frequency radiation is of interest, numerical methods must accurately capture this part of the spectrum (which is often contaminated by spurious oscillations due to steep gradients in fields around rupture fronts and wavefronts).

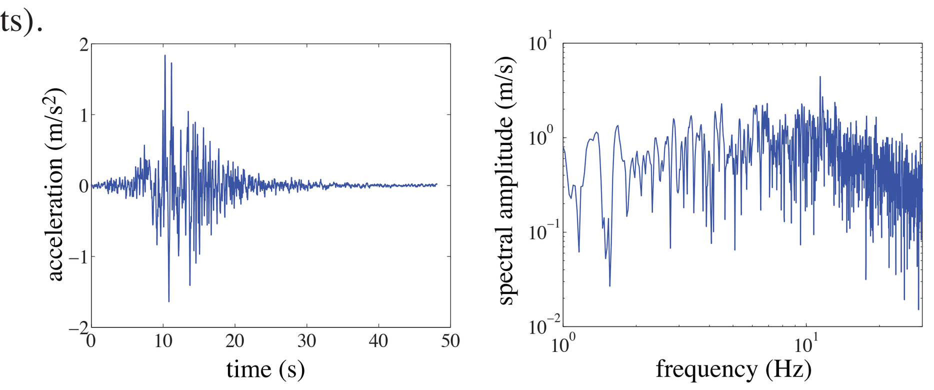

(above) Example of strong motion record at 2 km from fault in 1992 Landers earthquake (Lucerne Valley, N component). Fourier spectrum of acceleration is flat between 1 and 10 Hz, suggesting a process that excites waves over a broad range of frequencies. (right) LiDAR and profilometer measurements of fault surface roughness, showing how faults are rough at all scales [Power and Tullis, 1991; Renard et al., 2006; Sagy et al., 2007] in a self-similar manner: amplitude-to-wavelength ratio of roughness, γ, is independent of scale of observation. Faults are rougher in direction perpendicular to slip ($\gamma=10^{-2}$) than parallel to slip ($\gamma=10^{-3}$).

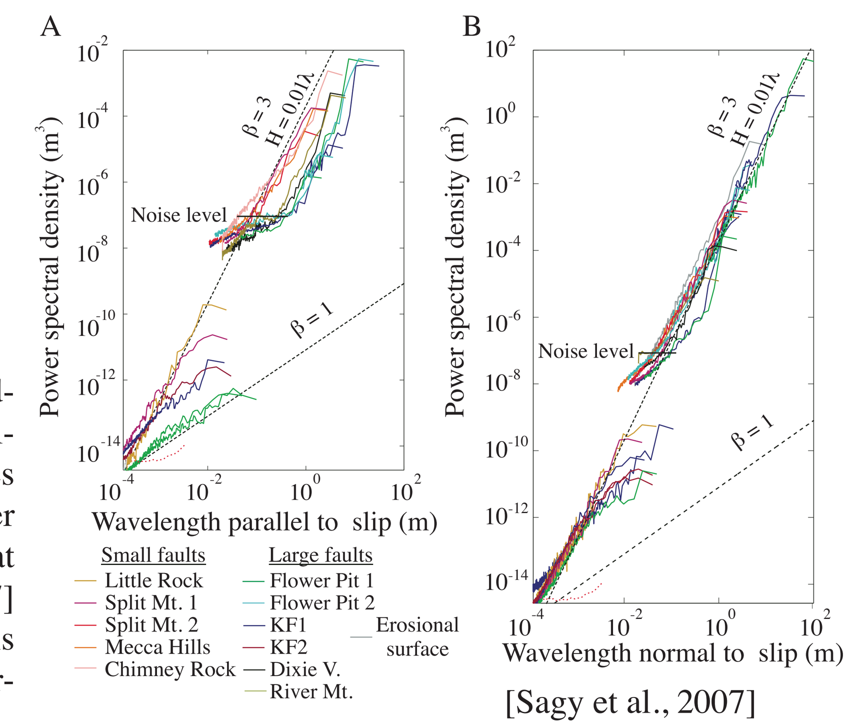

[Sagy et al., 2007]

Finite Difference Method with Coordinate Mapping

Governing Equations

momentum conservation and Hooke's law as (hyperbolic) system of first order PDEs (antiplane case with constant material properties for simplicity)

$$\frac{\partial}{\partial t}\begin{bmatrix} v_z \\ \sigma_{xz} \\ \sigma_{yz}\end{bmatrix} + \begin{bmatrix} 0 & -c^2/\mu & 0 \\ -\mu & 0 & 0 \\ 0 & 0 & 0\end{bmatrix}\frac{\partial}{\partial x}\begin{bmatrix} v_z \\ \sigma_{xz} \\ \sigma_{yz}\end{bmatrix} + \begin{bmatrix} 0 & 0 & -c^2/\mu \\ 0 & 0 & 0 \\ -\mu & 0 & 0\end{bmatrix}\frac{\partial}{\partial y}\begin{bmatrix} v_z \\ \sigma_{xz} \\ \sigma_{yz}\end{bmatrix} = \begin{bmatrix} 0 \\ 0 \\ 0\end{bmatrix}$$

or simply $\frac{\partial q}{\partial t} + A\frac{\partial q}{\partial x} + B\frac{\partial q}{\partial y} = 0$ or $\frac{\partial q}{\partial t} + \frac{\partial F}{\partial x} + \frac{\partial G}{\partial y} = 0$

WENO Reconstruction and Conservative Differencing

Strategy: Approximate spatial derivatives using nearby stencils (set of grid points) in which solution is smoothest. Avoid differentiation across discontinuitities (causes oscillations!). Consider 1D case (2D and 3D treated dimension by dimension):

1. discretize in space, defining point values as $q_i(t)= q(x_i,t)$ on mesh $\{x_i\}=\{i\Delta x\}$
2. write conservative difference formula $\frac{\partial q}{\partial t} + \frac{\partial F}{\partial x} = 0 \rightarrow \frac{\partial q_i}{\partial t} + \frac{F_{i+1/2} - F_{i-1/2}}{\Delta x} = 0$
3. evaluate $F_i=F(q_i)$ (at grid points)
4. reconstruct (approximate) $F_{i+1/2}$ and $F_{i-1/2}$ using values of $\{F_i\}$ as follows (for $F_{i+1/2}$)

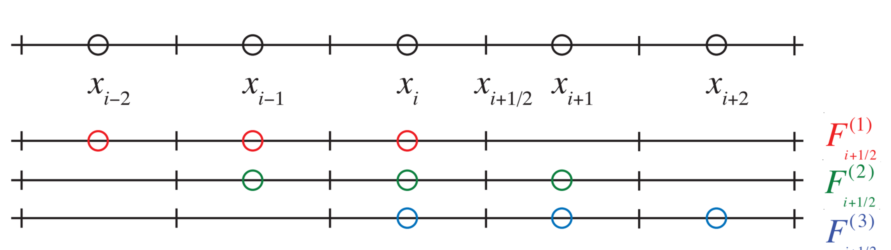

a. form three alternative reconstructions, using three different stencils

b. evaluate "smoothness indicator" for each stencil and assign weight ω to associated reconstruction (small weights for stencils crossing discontinuities or steep gradients in q, large weights if solution is smooth inside stencil)

c. form weighted linear combination of alternative reconstructions

$$F_{i+1/2} = \omega_1 F^{(1)}_{i+1/2} + \omega_2 F^{(2)}_{i+1/2} + \omega_3 F^{(3)}_{i+1/2}$$

Wave Decomposition and Upwinding

Notice that stencils are biased to left, which is appropriate for waves travelling from left (upwind) to right (downwind). Similar treatment for waves travelling from right to left. But we have waves propagating in both directions, so we must decompose fields into these waves and identify associated wave speeds. Again consider 1D case.

Diagonalize A: $\frac{\partial q}{\partial t} + A\frac{\partial q}{\partial x} = 0 \quad \rightarrow \quad \frac{\partial (Rq)}{\partial t} + \left(RAR^{-1}\right)\frac{\partial (Rq)}{\partial x} = 0$

Eigenvalues are wave speeds, dot products of eigenvectors with q (Riemann invariants) transported by waves:

$$RAR^{-1} = \begin{bmatrix} +c & 0 & 0 \\ 0 & -c & 0 \\ 0 & 0 & 0\end{bmatrix}$$

$\sigma_{xz} - (\mu/c)v_z$ propagates to right at speed $+c$

$\sigma_{xz} + (\mu/c)v_z$ propagates to left at speed $-c$

μ/c is shear impedence, and these are stress changes carried by plane S waves.

Split A into left- and right-going waves as $A=A^+ + A^-$, where

$$A^+ = R^{-1}\begin{bmatrix} +c & 0 & 0 \\ 0 & 0 & 0 \\ 0 & 0 & 0\end{bmatrix}R \quad \text{and} \quad A^- = R^{-1}\begin{bmatrix} 0 & 0 & 0 \\ 0 & -c & 0 \\ 0 & 0 & 0\end{bmatrix}R$$

Now split $F=Aq$ into left- and right-going waves as $F=F^+ + F^-$, and perform upwind-biased reconstruction of F^+ (biased to left) and F^- (biased to right).

Boundary Conditions

We use similar wave decomposition when applying boundary conditions. Use one-sided reconstructions near boundaries (and faults). Preserve Riemann invariants (as calculated by finite difference solution of PDEs) propagating from medium into boundary, set amplitudes of outward propagating waves to satisfy boundary conditions. For example, consider 1D case with fault at x=0.

1. update all fields with finite difference solution of PDEs
2. preserve value of Riemann invariants propagating into fault

$$\sigma^-_{xz} - (\mu/c)v^-_z = \sigma^{-,FD}_{xz} - (\mu/c)v^{-,FD}_z \qquad \sigma^-_{xz} = \sigma^+_{xz} = \tau - \tau_0,\ V = v^+_z - v^-_z$$

$$\sigma^+_{xz} + (\mu/c)v^+_z = \sigma^{+,FD}_{xz} + (\mu/c)v^{+,FD}_z \qquad \phi = \frac{1}{2}\left[\left(\sigma^{+,FD}_{xz} + \sigma^{-,FD}_{xz}\right) + (\mu/c)\left(v^{+,FD}_z - v^{-,FD}_z\right)\right]$$

$$\Rightarrow \tau = \tau_0 - (\mu/2c)V + \phi$$

3. solve together with friction law: $\tau = f(V)\sigma$

Coordinate Mapping For Irregular Geometries

Irregular geometries are typically handled using finite element methods, which may suffer from numerical oscillations and often require special treatment of nonphysical hourglass modes. But finite difference methods (like WENO) can also be used via a global mapping between irregular physical domain and Cartesian (rectangular) computational domain. Governing equations are transformed and solved in computational domain.

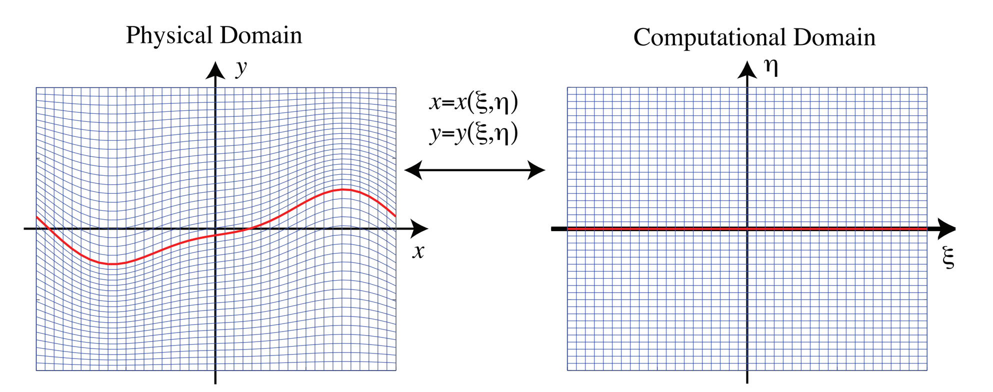

Transform governing equation using chain rule:

$$\left(x_\xi y_\eta - x_\eta y_\xi\right)\frac{\partial q}{\partial t} + \frac{\partial\left(y_\eta F - x_\eta G\right)}{\partial \xi} + \frac{\partial\left(-y_\xi F + x_\xi G\right)}{\partial \eta} = 0$$

(with $x_\xi = \partial x/\partial\xi$, etc.)

1D Test: Incident S wave (boxcar shape) on rate-and-state fault, comparing nonlinear WENO reconstruction (adaptive weighting of stencils) and upwind central reconstruction (all stencils have constant weights): (top) prior to wave reaching fault, (bottom) after wave reaches fault and induces slip.

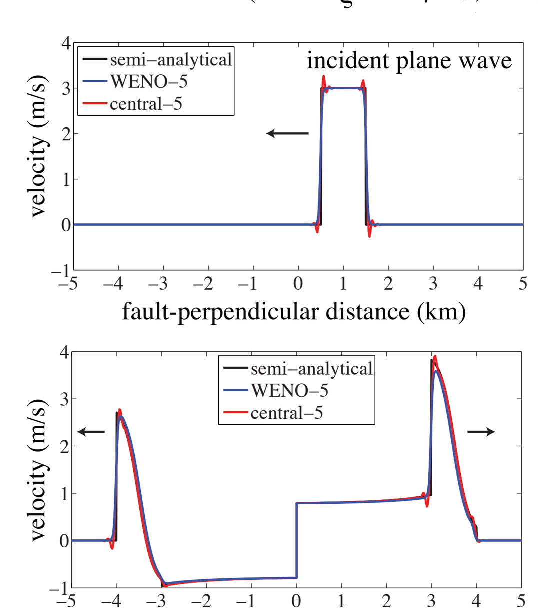

Dynamic Ruptures on Rough Faults

How does roughness affect rupture propagation? What are characteristics of high frequency ground motion and how are they related to amplitude-to-wavelength ratio of roughness, γ? Can contribution from different roughness wavelengths be isolated?

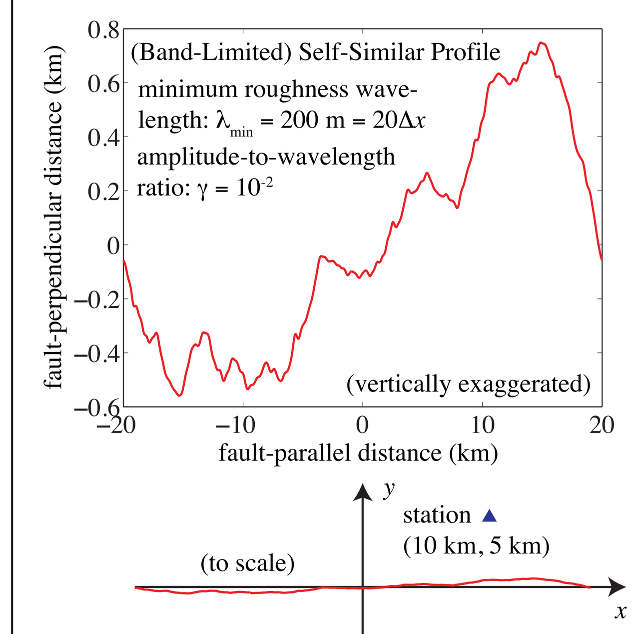

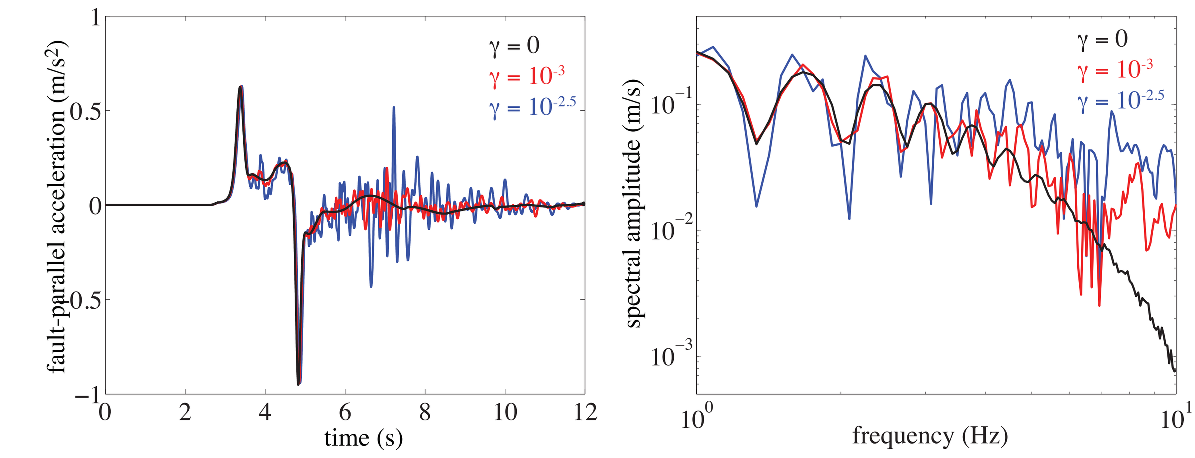

We modeled plane strain ruptures on rough faults with rate-and-state friction featuring strong dynamic weakening. (above), (below), and (right) Results from band-limited self-similar profile. Note large changes in normal and shear stress on fault. Changes will be even more extreme when shorter wavelength roughness is modeled.

Caution: While these figures show only minor perturbations to rupture process at $\gamma=10^{-3}$, *this may change when using smaller cut-off wavelength!*

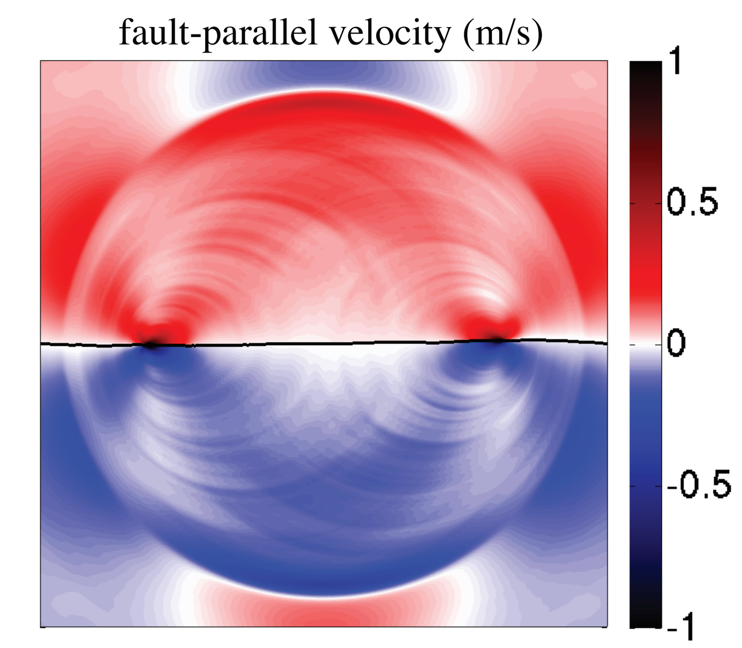

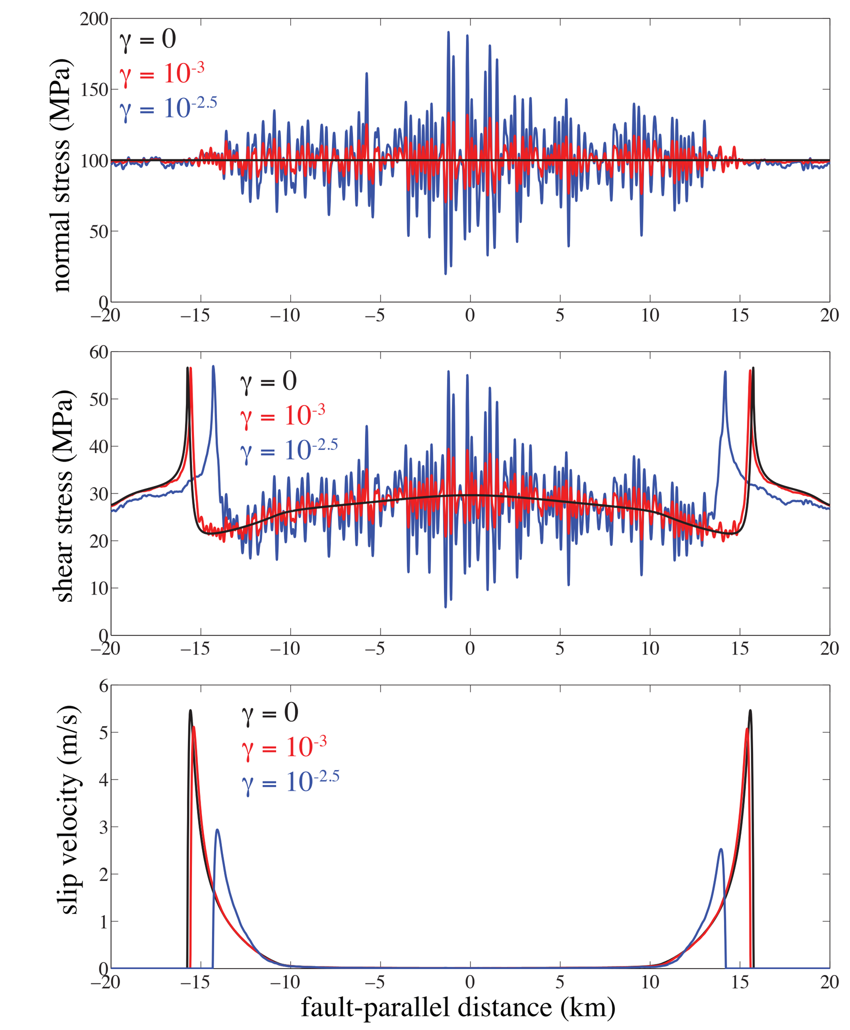

Single Fourier Mode Profiles

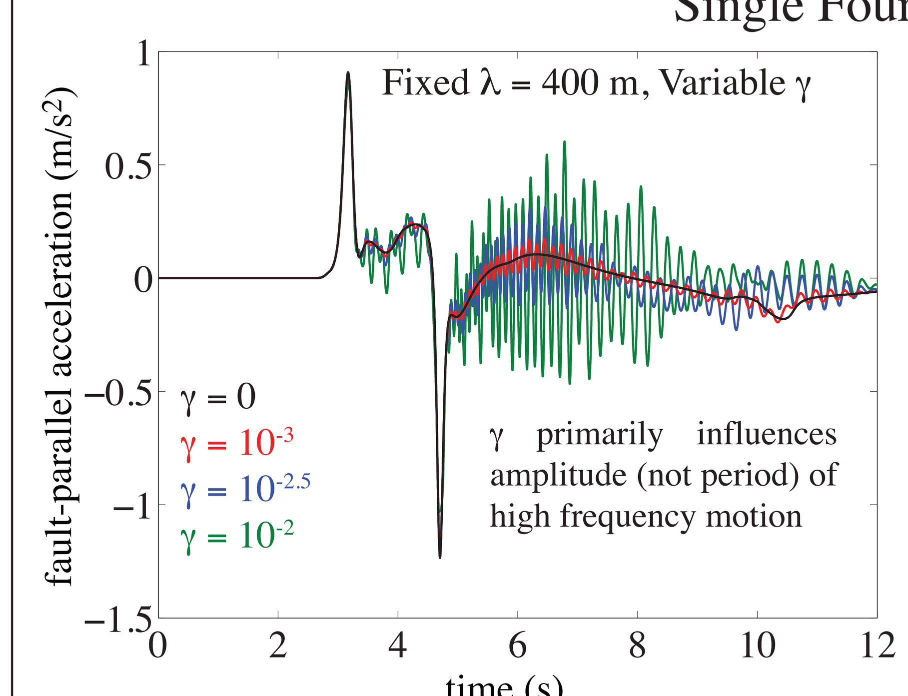

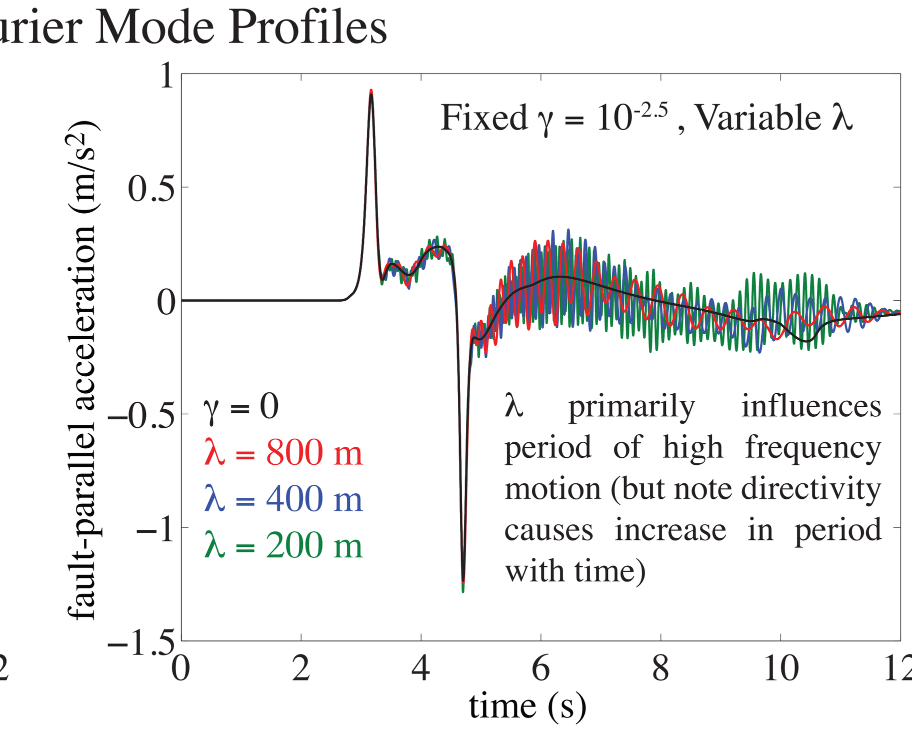

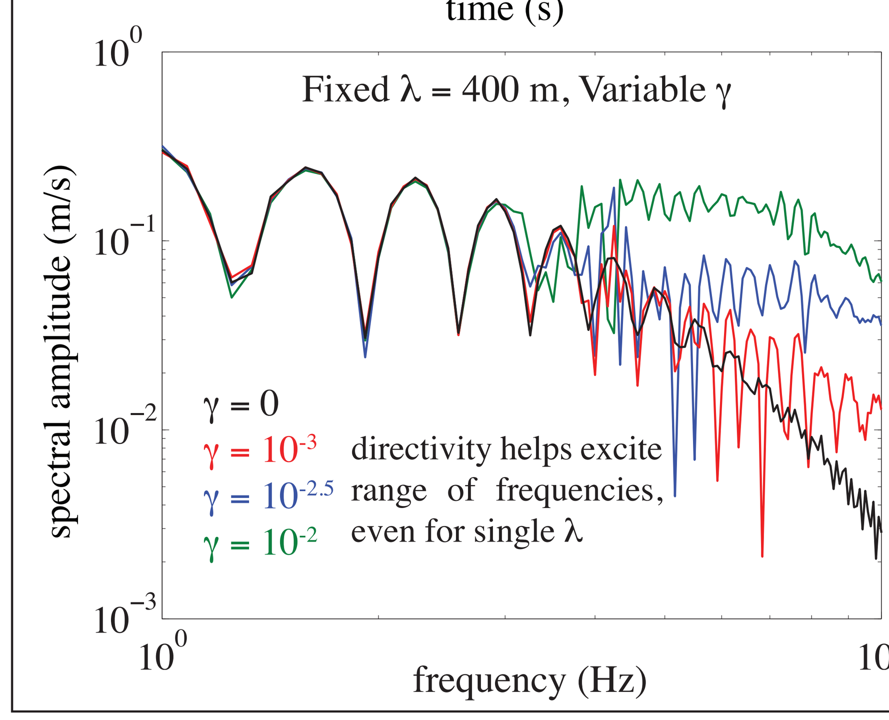

(left) and (above) Results from single Fourier mode profile, to separate effects of amplitude-to-wavelength ratio, γ, and wavelength, λ. A single roughness wavelength does not manifest as a distinct peak in the Fourier spectrum of ground motion due to directivity.

travel time difference between waves emitted at A and B:

$$\Delta t \approx \frac{\lambda}{c_s}\left(\frac{c_s}{v_r} + \frac{w}{r}\right)$$

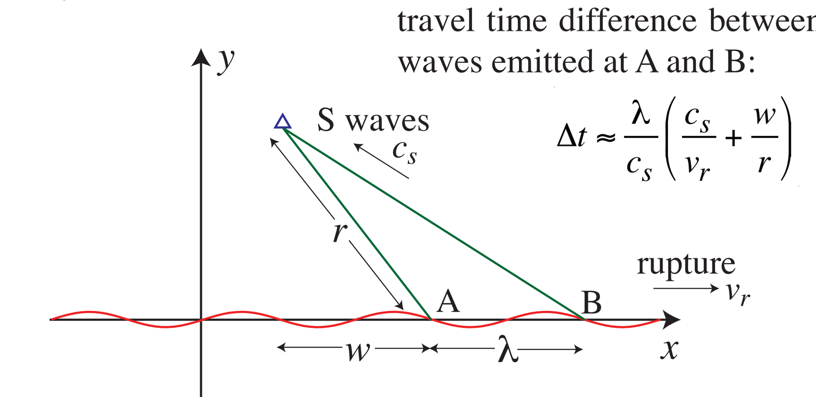

AGU 2008